Dentate gyrus–CA3 glutamate release/NMDA transmission mediates behavioral despair and antidepressant-like responses to leptin

Xuezhen Wang[1,2], **Di Zhang**[1], and **Xin-Yun Lu**[1,*]

[1]Department of Pharmacology, The University of Texas Health Science Center at San Antonio, San Antonio, TX 78229, USA

[2]Institute for Metabolic and Neuropsychiatric Disorders, Binzhou Medical University, China

Abstract

Compelling evidence supports the important role of the glutamatergic system in the pathophysiology of major depression and also as a target for rapid-acting antidepressants. However, the functional role of glutamate release/transmission in behavioral processes related to depression and antidepressant efficacy remains to be elucidated. In this study, glutamate release and behavioral responses to tail suspension, a procedure commonly used for inducing behavioral despair, were simultaneously monitored in real time. The onset of tail suspension stress evoked a rapid increase in glutamate release in hippocampal field CA3, which declined gradually after its offset. Blockade of NMDA receptors by intra-CA3 infusion of MK-801, a non-competitive NMDA receptor antagonist, reversed behavioral despair. The CA3 was innervated by granule neurons expressing the leptin receptor (LepRb) in the dentate gyrus (DG), representing a subpopulation of granule neurons that were devoid of stress-induced activation. Leptin treatment dampened tail suspension-evoked glutamate release in CA3. On the other hand, intra-CA3 infusion of NMDA blocked the antidepressant-like effect of leptin in reversing behavioral despair in both the tail suspension and forced swim tests, which involved activation of Akt signaling in DG. Together, these results suggest that the DG-CA3 glutamatergic pathway is critical for mediating behavioral despair and antidepressant-like responses to leptin.

Keywords

leptin; glutamate release; NMDA; behavioral despair; dentate gyrus; CA3

INTRODUCTION

Mounting evidence suggests dysfunction of the glutamatergic system as a major pathological feature in stress-related mental illnesses and a potential target for pharmacological intervention [1-3]. A number of studies have shown that acute exposure to

[*] Correspondence: Xin-Yun Lu, M.D., Ph.D. Department of Pharmacology University of Texas Health Science Center at San Antonio 7703 Floyd Curl Drive San Antonio, TX 78229, USA Phone: 210-567-0803 Fax: 210-567-4303 lux3@uthscsa.edu.

various types of stress increases glutamate release in limbic areas [4-7] and enhances depolarization-evoked release of glutamate in synaptosomes isolated from these brain regions [8-11]. In contrast, chronic administration of traditional antidepressants reduces depolarization-evoked and stress-induced release of glutamate [8, 12]. However, the functional role of glutamate release/transmission in behavioral processes related to depression and antidepressant efficacy is poorly understood.

Accumulating evidence strongly supports hippocampal dysfunction in major depression [13-15]. Brain imaging studies show hippocampal atrophy in patients with major depression [16, 17] and changes in hippocampal activity linking to the response to antidepressant treatments [18]. Preclinical studies indicate that the hippocampus is a structure sensitive to the effects of stress and stress hormones [19] and also a site where antidepressants elicit behavioral effects [20-24]. Thus, the hippocampus has been proposed to be a neural substrate that mediates the expression of depressive behaviors and antidepressant actions. The hippocampus consists of distinct subregions, including the dentate gyrus (DG), CA3 and CA1, that are interconnected by a tri-synaptic circuit relaying glutamatergic synaptic transmission. Each subregion of the hippocampus has distinct physiological roles and differential responsiveness to stress. Available evidence suggests that CA3 pyramidal neurons are particularly vulnerable to stress. Prolonged exposure to restraint and other forms of stress cause atrophy of dendritic trees of CA3 neurons in different species [25-27].

The CA3 is innervated by glutamatergic afferents originating primarily from granule neurons in DG [28]. Thus, intrinsic and extrinsic factors that modulate activity of DG granule neurons would be critical in controlling glutamate release in CA3. We have previously shown that the DG is a functional target of leptin, an adipocyte-derived hormone with antidepressant-like properties [21, 22, 29-31]. Direct infusion of leptin into DG produces antidepressant-like effects [22], whereas deletion of the leptin receptor, LepRb, in this region induces depression-like behaviors [32]. On the other hand, DG granule neurons can be activated by exposure to a variety of stressors [33-38]. However, whether there is a causal link between glutamate release and stress-induced depressive behaviors and whether the antidepressant-like effects of leptin involve modulation of the DG-CA3 glutamatergic pathway remain to be answered. .

Among the various animal models, the "behavioral despair" paradigms incorporating inescapable stress, i.e. the tail suspension and forced swim tests, are the most commonly used for assessing antidepressant activity. Behavioral despair in these two models is reduced by antidepressants and facilitated by exposure to stress [39, 40]. Surprisingly, to date there has been very little attention devoted to these two behavioral despair models for investigating the effects of stress and antidepressants on glutamate release and identifying a causal relationship between glutamate release and behavioral effects. In this study, we monitored glutamate release in CA3 and behavioral despair and explored their relationships. Moreover, we examined the effect of stress on LepRb neurons in DG and the possibility of dampening stress-evoked glutamate release/transmission in CA3 as a mechanism underlying antidepressant responses to leptin.

METHODS and MATERIALS

Animals

Adult male C57BL/6J mice (The Jackson Laboratory, Bar Harbor, MA) were housed in groups of five under a 12-h light–dark cycle (lights on at 7:00 am) with *ad libitum* access to food and water except during the behavioral tests. Animals were allowed to acclimate for at least 1 week before beginning the experiments. All animal procedures were conducted in accordance with NIH guidelines and approved by the Institutional Animal Care and Use Committee of the University of Texas Health Science Center at San Antonio.

Production of the LepRb-tdTomato reporter mice—In order to reveal the distribution of LepRb neurons and their projections, LepRb-IRES-Cre mice were crossed with the reporter Gt(ROSA)26Sor[tm14(CAG-tdTomato)] mice that express tdTomato in a Cre-dependent manner (The Jackson Laboratory). LepRb-IRES-Cre mcie were generated with an IRES-NLS-Cre cassette "knocked in" into the region immediately 3′ to the LepRb stop codon [41]. Cre recombinase expression in this line of mice is restricted to LepRb-expressing cells. The Gt(ROSA)26Sor[tm14(CAG-tdTomato)] reporter mice were engineered to contain a loxP-flanked transcriptional STOP cassette preceding the red fluorescent protein variant (tdTomato) inserted into the *Gt(ROSA)26Sor* locus. When bred with LepRb-IRES-Cre mice, the resulting offspring had the STOP cassette deleted by Cre-mediated recombination, enabling the expression of downstream tdTomato coding sequences in LepRb-expressing cells (LepRb-tdTomato). The Gt(ROSA)26Sor[tm14(CAG-tdTomato)] allele and LepRb[cre] allele were determined by PCR genotyping with the primers 5'-GGC ATT AAA GCA GCG TAT CC-3' and 5'-CTG TTC CTG TAC GGC ATG G-3' and the primers 5'-GCG GTC TGG CAG TAA AAA CTA TC-3'and 5'-GTG AAA CAG CAT TGC TGT CAC TT-3'.

Drugs

Recombinant mouse leptin (R&D Systems, Minneapolis, MN) was dissolved in sterile saline at a concentration of 1.0 mg/ml and administered intraperitoneally (i.p.) at a dose of 1.0 mg/kg body weight. For intra-CA3 injections, N-methyl-D-aspartic acid (NMDA) and l5R, 10S)-(+)-5-methyl-10,11-dihydro-5H-dibenzo[a,d]cyclohepten-5,10-imine hydrogen maleate (MK-801; Sigma-Aldrich, St Louis, MO) were dissolved in Dulbecco's phosphate-buffered saline and injected at a dose of 0.1 nmol/μl for NMDA and a dose of 1 μg/μl for MK-801. For intra-DG injection, Akt inhibitor VIII (1,3-dihydro-1-(1-((4-(6-phenyl-1H-imidazo[4,5-*g*]qui-noxalin-7-yl)phenyl)methyl)-4-piperidinyl)-2H-benzimidazol-2-one), an isozyme-selective Akt inhibitor specific for Akt1/2 (Calbiochem, La Jolla, CA), was dissolved in DMSO (Sigma) and injected at a dose of 3.0 μg/μl. L-glutamic acid monosodium salt hydrate and ascorbic acid were purchased from Sigma and dissolved in distilled water in stock concentrations of 5 mM and 100 mM for biosensor calibration, respectively.

Glutamate concentration measurement

Glutamate biosensors enable the monitoring of real-time changes in extracellular glutamate concentrations in the brain of freely moving animals. Biosensors, guide cannula and head mounts, potentiostat, and recording/processing software were purchased from Pinnacle

Technology (Lawrence, KS). Guide cannula for biosensor recording were implanted into hippocampal field CA3 (AP: –2.8 mm, ML: 3.0 mm, DV: –2.5 mm from bregma). The guide cannula hubs were fixed to the skull with a head mount that was sealed with dental acrylic resin and secured with four stainless steel bone screws. Following the surgery, a stainless steel obturator was inserted into the cannula to prevent occlusions. After 7 days of recovery from surgery, mice were placed in the recording chamber for habituation to experimental protocol conditions and handled for 3-4 times daily for three days before insertion of a biosensor (Model 8401). The glutamate biosensor incorporates an enzyme-coated microelectrode that measures oxidation currents of hydrogen peroxide generated by conversion of glutamate to alpha-ketoglutaraldehyde and hydrogen peroxide by glutamate oxidase. Before implanting, each biosensor was calibrated *in vitro* at 37°C with five 10 μM increments of glutamate (from 0 to 50 μM) in phosphate buffered saline (PBS; 150 mM NaCl, 8.7 mM Na_2HPO_4, 16 mM KH_2PO_4, pH 7.4) to verify glutamate sensitivity, followed by a single addition of the electron donor ascorbic acid (250 μM) to verify specificity. The biosensor with 1-mm long active area was inserted through the guide cannula into CA3 area the night before the experiment procedure. The biosensor was connected to a four-channel potentiostat via an electrically shielded flexible cable. The protentiostat transmitted signals to a paired bluetooth USB dongle that interfaces with Pinnacle's Sirenia Acquisition software for data recording. Following biosensor implantation, current trace recording was initiated, and the biosensor was allowed to equilibrate overnight before any experimental procedures. When the baseline current was stable, mice were subjected to tail suspension or administered with leptin (1.0 mg/kg) or saline 30 min prior to the tail suspension procedure. Changes in glutamate levels before, during and after the tail suspension test (TST) were recorded by glutamate biosensors. Electrochemical data were collected at 1 Hz. At the end of recording session, mice were disconnected from the potentiostat, and the biosensor was removed for post-recording calibration as described above. To convert the recorded currents to glutamate concentrations, linear regression was performed on calibration data.

Behavioral tests

Behavioral despair tests—Behavioral despair can be induced by tail suspension or forced swim. Animals are subjected to inescapable stress of being suspended by their tail or being forced to swim in a narrow cylinder of water. After initial attempts to escape by engaging in vigorous movements or swimming/climbing, the animals develop a characteristic immobile posture. This immobility is thought to reflect a state of behavioral despair, which is selectively attenuated by antidepressant drugs [39, 40]. For the TST, the apparatus was constructed of a wooden box (30×30×30 cm) with an open front. A horizontal bar was placed 1 cm from the top and a vertical 9 cm bar hanging down in the center. Mice were individually suspended by the tail to the vertical bar with adhesive tape affixed 2 cm from the tip of the tail. The animal's behavior was recorded for 6 min. The immobility and escape oriented behaviors were scored by a trained observer who was blind to the treatments. The automated tail suspension apparatus consisted of a lab support stand holding a strain gauge. Each mouse was suspended by the tail using adhesive tape to a ventricle bar connected to the strain gauge. The strain gauge detected movements of the mouse and the electrical signals were transmitted to a central unit. A histogram of real-time movements

during the 6-min test was created automatically. A video analysis of the TST was performed simultaneously and evaluated as described above. For the forced swim test (FST), mice were placed in a clear Plexiglas cylinder (25 cm high; 10 cm in diameter) filled to a depth of 15 cm with 24°C water. Animals' behavior in a 6-min test session was recorded. The first 2 min were designated as a habituation period, and the duration of immobility was measured during the last 4 min as described elsewhere [21, 42]. Immobility in this test was defined as the absence of any limb or body movements, except those caused by respiration.

Locomotor activity—Mice were placed in an open field arena (40 ×40 × 40 cm) and allowed to freely explore for 30 min. A CCD camera was mounted above the open box for recording locomotor activity. The total distance traveled was measured using a Noldus EthoVision 3.0 system (Noldus Information Technology Inc., Leesburg, VA).

Stereotaxic surgery and microinjection

Mice were anesthetized and implanted bilaterally with a guide cannula (Plastics One, Roanoke, VA) into CA3 or DG using a procedure described previously [43]. The skull surface was first coated with Kerr phosphoric acid gel etchant (Kerr, Orange, CA). After the guide cannula was inserted into CA3 (coordinates: -2.8 mm posterior, ±3.0 mm lateral, and -2.5 mm ventral to the bregma) or DG (coordinates: -2.1 mm posterior, ±1.5 mm lateral, and -1.2 mm ventral to the bregma), Kerr Prime was applied onto the skull and cannula surface. Then adhesive was brushed on top of the primer layer and light cured for 45 sec with the VALO curing light (Ultradent Products Inc., St Louis, MO). Finally, the dental cement was used to fill the area around the cannula and a dummy cannula was inserted into the guide cannula to maintain the cannula patency. Animals were individually housed, handled daily, and allowed to recover for 7 d after surgery.

All intra-nucleus microinjections were performed on conscious, unrestrained, and freely moving mice in their home cage. On the experimental day, a 33-gauge stainless steel injector connected to a 5-μl syringe was inserted into the guide cannula and extended 1 mm beyond the tip. Drugs or vehicle were infused bilaterally in a volume of 0.5 μl over 2 min. An additional 5 min was allowed for diffusion and prevention of backflow through the needle track before the injector was withdrawn. For intra-CA3 injection of MK-801, eighteen mice were weighed and counter-balanced into two groups. Mice received bilateral intra-CA3 infusion of MK-801 (1.0 μg) or vehicle at 30 min prior to the TST (MK-801, n = 9; Vehicle, n = 9) or locomotion test (MK-801, n = 4; Vehicle, n = 4). For the experiments involving intra-CA3 NMDA injections, mice were divided into four different treatment groups, including vehicle+saline, vehicle+leptin, NMDA+leptin and NMDA+saline. Mice first received bilateral intra-CA3 infusion of NMDA (0.1 nmol) or vehicle, and 30 min later were given i.p. injection of leptin (1.0 mg/kg) or saline. Thirty-min after leptin injection, mice were subjected to the TST (vehicle+saline, n = 8; vehicle+leptin, n = 9; NMDA+leptin, n = 8; NMDA+saline, n = 8), FST (vehicle+saline, n = 9; vehicle+leptin, n = 9; NMDA +leptin, n = 8; NMDA+saline, n = 9), or locomotion test (vehicle+saline, n = 9; vehicle +leptin, n = 8; NMDA+leptin, n = 9; NMDA+saline, n = 8). For the experiments involving intra-DG injection of Akt inhibitor VIII (Akt-i), mice were divided into four different treatment groups: vehicle+saline, vehicle+leptin, Akt-i+saline, and Akti+leptin. Mice first

received intra-DG infusion of Akt-i (3.0 μg) or vehicle, and 30 min later were injected with leptin (1.0 mg/kg, i.p.) or saline. Behavioral tests including the TST (vehicle+saline, n = 9; vehicle+leptin, n = 15; Akt-i/3.0 μg+saline, n = 7; Akt-i/3.0 μg+leptin, n = 13), FST (vehicle +saline, n = 8; vehicle+leptin, n = 8; Akt-i/3.0 μg+saline, n = 7; Akt-i/3.0 μg+leptin, n = 12) or locomotion test (vehicle+saline, n = 8; vehicle+leptin, n = 12; Akti/3.0 μg+saline, n = 7; Akt-i/3.0 μg+leptin, n = 8) were performed 30 min after leptin injection.

Cannula verification

For verification of the intra-CA3 and intra-DG cannula, mice were injected with 0.5 μl India ink via an injector under anesthesia followed by decapitation. The brains were then removed and frozen in a dry ice-isopentane bath (−35°C). For verification of the glutamate biosensor placement in CA3, mice were perfused with 4% paraformaldehyde in PBS and cryoprotected in 30% sucrose solution. Brains were sectioned in the coronal plane with a cryostat at 20 μm. The cannula placement was determined under a dissecting microscope according to the mouse brain atlas [44]. Animals with misplacement of cannula were excluded from data analysis.

Western blot assay

Mice were decapitated rapidly at 30 min after i.p. injection of leptin. The hippocampi were dissected out and homogenized in lysis buffer (50 mM HEPES pH 7.6, 1% triton X-100, 150 mM NaCl, 20 mM sodium pyrophosphate, 20 mM b-glycerophosphate, 10 mM NaF) containing a mixture of phosphatase inhibitors (leupeptin, aprotinin, sodium orthovanadate, phenylmethylsulfonyl fluoride, Ser/Thr phosphatase inhibitor mixture, Tyr phosphatase inhibitor mixture). A total amount of 40 μg protein was separated by SDS-PAGE, and transferred to a nitrocellulose membrane. The membrane was blocked in a blocking buffer (0.01 M Tris-buffered saline, 0.01M Tris base, 0.9% NaCl with 1% dry milk and 0.1% Tween 20) followed by incubation with mouse anti-Akt (1:1000; Invitrogen, Carlsbad, CA) and rabbit anti-pAkt^{Thr308}, pAkt^{Ser473} or Akt antibodies (1: 1000, Cell Signaling Technology Inc., Danvers, MA) diluted in a solution of 1% bovine serum albumin and 0.1% Tween-20 in Tris-buffered saline overnight at 4°C. Horseradish peroxidase-conjugated anti-mouse or anti-rabbit immunoglobulin G was used as secondary antibodies (1:5000, Cell Signaling). Signals were detected by enhanced chemilluminescence (Thermo Scientific, Rockford, IL). Quantification of Western blotting was performed using ImageJ software with normalization to total protein levels.

Immunohistochemistry

To examine expression of LepRb in granule neurons in DG, LepRb-tdTomato mice were transcardially perfused with 4% paraformaldehyde. The brains were removed, post-fixed overnight, and then cryoprotected in 30% sucrose and cut into 40-μm coronal sections. Immunohistochemistry was performed to detect Prox1, a marker of granule neurons, in LepRbtdTomato neruons. Briefly, sections were rinsed three times in PBS, and incubated in blocking buffer (1% BSA, 3% goat serum, 0.3% triton X-100 in PBS) for 1 h. The sections were then incubated with mouse anti-Prox1 antibody (1:1000; Millipore, Billerica, MA). After washing in PBS, sections were incubated for 4 h with fluorescent secondary antibodies: Alexa Fluor 488 goat anti-mouse IgG (1:400, Molecular Probes, Eugene, OR).

Finally, the sections were washed in PBS, mounted onto poly-lysine coated glass slides, and coversliped with fluorescence mounting medium and visualized using an Olympus FV1000 confocal microscope.

To determine stress-induced c-Fos expression in LepRb-tdTomato mice, mice were subjected to 10 min of tail suspension or 10 min of forced swim. Forty-five5 min after stress mice were perfused and processed as described above. The brain sections were incubated with rabbit anti-c-Fos (1:1000; Calbiochem, San Diego, CA) antibody for 48 h at 4°C, followed by incubation with horseradish peroxidase-conjugated goat anti-rabbit antibody (1:400, Progema, Madison, WI) for 1 h. Then, the tissue sections were incubated with avidin/biotin complex followed by 3,3-diaminobenzidine substrate (Vector Laboratories, Burlingame, CA).

Statistical analysis

Results are expressed as mean ± standard error of the mean (SEM). Two-way ANOVA was used for the analysis of behavioral effects of NMDA, Akt inhibitor VIII and leptin in the TST and FST, and one-way or two-way ANOVAs with repeated measures were used for the analysis of current data, glutamate concentrations, rate of change in glutamate concentrations and locotmotion, followed by *post hoc* comparisons (Bonferroni/Dunn or Tukey/Kramer for unequal n). Two-tailed *t*-test was used for the rest of the experiments.

RESULTS

Simultaneous monitoring glutamate release in CA3 and behavioral despair in freely moving mice

Monitoring behavioral activity and real-time changes in extracellular glutamate levels would enable us to establish the temporal relationship between glutamate release and behavioral changes. A microelectrode biosensor was used for real-time measuring of extracellular glutamate concentrations in CA3 in freely behaving mice during the tail suspension behavioral despair test. The high temporal resolution of biosensor allowed the monitoring of the physiological time course of glutamate responses. We found that extracellular glutamate concentrations in CA3 were rapidly increased after the onset of tail suspension, peaked at the end of 6-min session, and declined gradually to baseline within 30 min after its offset (Figure 1A, B). During the 6-min tail suspension, behavioral responses were automatically recorded by a strain gauge transducer. The histogram of real-time movements showed that struggle activity was stronger at the beginning of 6-min tail suspension when the rate of change in glutamate levels was high in CA3 (Figure 1A). Immobile episodes, reflecting a state of behavioral despair, became more frequent and longer toward the end of tail suspension along extracellular accumulation of glutamate in CA3 (Figure 1A). Statistical analyses indicated that there were significant effects of time on extracellular glutamate concentrations ($F_{(36, 111)} = 6.758$, $p < 0.0001$) and rate of change in extracellular glutamate concentrations ($F_{(18, 57)} = 6.531$, $p < 0.0001$). It appeared that the increase in the rate of change in glutamate concentrations occur only during tail suspension (Figure 1B).

Blockade of NMDA receptors in CA3 reverses behavioral despair

Excessive glutamate release induced by tail suspension is proposed to result in overactivation of NMDA receptors [45, 46]. To determine whether NMDA receptor activation is responsible for behavioral despair, mice received intra-CA3 infusion of MK-801 (1.0 μg), a non-competitive NMDA antagonist, 30 min prior to tail suspension. MK-801 significantly reduced behavioral despair, as indicated by decreased immobility time (Figure 2A). There was no significant main effect of MK-801 ($F_{(1, 90)} = 0.623$, $p > 0.1$) or interaction between MK-801 and time ($F_{(14, 90)} = 0.417$, $p > 0.5$) on locomotor activity, indicating that the effect of MK-801 on behavioral despair is not due to non-specific hyperlocomotion (Figure 2B). These findings suggest that NMDA receptor activation in CA3 may underlie the mechanisms of behavioral despair in the TST. The location of all the microinjection sites is summarized schematically in Figure 2C. Injection sites outside of the region were not included for statistical analyses.

CA3 receives glutamatergic inputs from LepRb-expressing granule neurons in DG

CA3 neurons receive massive glutamatergic inputs from granule neurons in DG. To reveal the distribution of LepRb neurons and their axonal projections, we generated a report line of mice that expressed the tdTomato fluorescent protein specifically in LepRb cells. This protein is among the brightest fluorescent proteins that are currently available [47]. It is uniformly distributed throughout the cells and their processes [48], allowing us to visualize dendrites and axonal projections. We found that LepRb-tdTomato cells were largely restricted to the granule cell layer in DG with sparse cells observed in CA3 (Figure 3A). LepRb-tdTomato was exclusively colocalized with Prox1, a granule neuron marker (Figure 3B). The axonal terminals of LepRb granule neurons were extended to CA3 (Figure 3A), suggesting that LepRb neurons participate in modulating CA3 activity.

LepRb granule neurons in DG are devoid of stress-induced activation

To determine whether LepRb granule neurons are activated by stress, c-Fos expression was examined in LepRb-tdTomato mice following exposure to tail suspension and forced swim for 10 min. c-Fos positive cells were seen in the granule cell layer of DG in mice exposed to tail suspension or forced swim. However, none of LepRb granule neurons in DG were found to be positive for c-Fos (Figure 3C). The absence of c-Fos in LepRb neurons in DG suggests that LepRb neurons represent a subpopulation of DG granule neurons that are devoid of stress activation.

Leptin inhibits stress-evoked glutamate release in CA3

The observation of LepRb granule neurons in DG projecting to CA3 suggests that leptin may modulate glutamate release in CA3 evoked by tail suspension. To test this possibility, mice received an i.p. leptin injection (1.0 mg/kg) 30 min before the TST and changes in extracellular glutamate levels in CA3 were monitored using microelectrode biosensors. There was a significant main effect of leptin treatment on extracellular glutamate concentrations during the 6-min TST ($F_{(1, 49)} = 18.883$, $p < 0.001$) and within 32 min after the onset of TST ($F_{(1, 231)} = 32.759$, $p < 0.001$). Tail suspension-evoked glutamate release in CA3 was significantly inhibited by leptin treatment (Figure 4). After cessation of tail

suspenstion stress, the increased glutamate levels returned to baseline within a shorter period of time in the leptin-treated group in comparison with the vehicle treatment (Figure 4A, B). Leptin-induced inhibition of rate of changes in extracellular glutamate levels occur largely within the first min of tail suspension (Figure 4C).

Activation of NMDA receptors in CA3 blocks the effects of leptin on behavioral despair

Next we attempted to determine whether inhibition of stress-evoked glutamate release in CA3 contributes to the antidepressant-like effects of leptin. Given the above-stated finding that blockade of NMDA receptors in CA3 reversed behavioral despair, we speculated that activation of NMDA receptors in this region would cancel out the effect of leptin-induced inhibition of glutamate release, thereby blocking the antidepressant-like behavioral action of leptin. To test this, mice received intra-CA3 infusion of 0.1 nmol NMDA at 30 min before leptin was administered (1.0 mg/kg, i.p.). The TST as well as the FST were performed at 30 min after leptin injection. The statistical analyses of immobility time revealed a significant main effect of leptin treatment ($F_{(1, 29)} = 5.784$, $p < 0.05$ for TST; $F_{(1, 31)} = 8.280$, $p < 0.01$ for FST), but not NMDA treatment ($F_{(1, 29)} = 2.120$, $p > 0.1$ for TST; $F_{(1, 31)} = 0.875$, $p > 0.1$ for FST). There was an approaching significant interaction between leptin and NMDA treatment in the TST ($F_{(1, 29)} = 3.709$, $p = 0.064$); and their interaction in the FST was significant ($F_{(1, 31)} = 8.609$, $p < 0.01$). *Post-hoc* analyses showed that leptin significantly decreased immobility time in both TST and FST ($p < 0.01$), and intra-CA3 NMDA treatment abolished the effect of leptin in both tests ($p < 0.05$) (Figure 5A). There was no significant main effect of treatments ($F_{(3, 450)} = 0.355$, $p = 0.786$) and interaction between treatments and time on locomotor activity ($F_{(42, 450)} = 0.588$, $p > 0.5$) (Figure 5B), supporting the specificity of the effects of leptin and NMDA on behavioral despair. The location of the microinjection sites is summarized in Figure 5C.

Akt signaling in DG is required for the effect of leptin on behavioral despair

Akt signaling in the hippocampus has been implicated in depression and the mechanisms of action of antidepressants [49]. Akt is one of the main LepRb intracellular signaling pathways [50]. Leptin, at an effective dose (1.0 mg/kg, i.p.) for antidepressant-like effect, induced Akt phosphorylation on Thr308 but not on Ser473 in the hippocampus at 30 min after administration, in temporal correlation with its behavioral effect (Figure 6A). To determine whether Akt signaling is involved in leptin actions in reversing behavioral despair, mice received intra-DG injection of Akt inhibitor VIII at 30 min prior to i.p. injection of leptin (1.0 mg/kg, i.p.). Immobility time was scored in the TST and FST 30 min after leptin injection. Statistical analyses indicated significant main effects of leptin treatment ($F_{(1, 43)} = 12.068$, $p < 0.001$) and Akt inhibitor VIII ($F_{(1, 43)} = 8.791$, $p < 0.05$) on immobility time in the TST and significant interactions between leptin and Akt inhibitor VIII treatments in both TST and FST ($F_{(1, 43)} = 5.295$, $p < 0.05$ for TST; $F_{(1, 31)} = 7.959$, $p < 0.01$ for FST). *Post-hoc* analyses revealed that leptin significantly decreased immobility time in both TST and FST ($p < 0.01$), and this effect was blocked by Akt inhibition ($p < 0.01$) (Figure 6B). Mice treated as described above were tested for locomotor activity and displayed no significant difference in total distance traveled between different treatment groups (Figure 6C). The location of the microinjection sites is summarized in Figure 6D.

DISCUSSION

Our studies indicate a key role for glutamate release/transmission in the CA3 field of the hippocampus in mediating behavioral despair and antidepressant responses. We demonstrated that behavioral despair was temporally correlated with stress-evoked glutamate increase in CA3 and reduced by blocking NMDA receptors, suggesting that glutamate release/NMDA transmission in CA3 could be an essential mechanism underlying behavioral despair. The CA3 glutamatergic terminals arise primarily from DG granule neurons, a functional target of leptin. One important finding of this study is that LepRb neurons in DG appeared to represent a subpopulation of granule neurons that are devoid of stress-induced activation. Dampening stress-evoked glutamate release/NMDA transmission in CA3 likely serves as a downstream mechanism underlying the effect of leptin in reversing behavioral despair, which involves activation of Akt signaling in DG. These findings suggest the importance of modulation of DG-CA3 glutamatergic transmission in behavioral despair and antidepressant-like responses to leptin.

A number of studies have shown that exposure to various stressors differing in intensity and duration increases glutamate concentrations in different limbic brain regions including the hippocampus [4-7, 51], whereas antidepressant treatments block depolarization- or stress-evoked glutamate release [8, 12, 52, 53]. Glutamate release in these studies was measured using *in vitro* synaptosomal [52, 53] and slide preparations [54] or *in vivo* microdialysis techniques [4-7, 51]. These findings have contributed to our knowledge of regulation of the glutamatergic system by stress and antidepressants. However, none of these studies were combined with behavioral analysis in an attempt to identify a causal relationship between glutamate release and antidepressant behavioral effects. In the present study, endogenous glutamate release was monitored in CA3 in real time using a highly sensitive and selective microelectrode biosensor with a fast response time (1 sec). Simultaneously, behavioral responses to tail suspension were automatically recorded. The episodes of immobility, reflecting behavioral despair, became more frequent and longer along with rapid and persistent increase in extracellular glutamate concentrations in CA3. Our results for the first time demonstrate the relevance of release and accumulation of glutamate to behavioral despair. Excessive release of glutamate would lead to spillover from synapses to extrasynaptic sites, where predominantly NMDA receptors are located [46, 55, 56]. We showed that blockade of NMDA receptors in CA3 was sufficient to reverse behavioral despair, suggesting that tail suspension-evoked excessive glutamate release and subsequent NMDA receptor activation in CA3 mediate the induction of behavioral despair. This is generally consistent with previous studies showing that glutamate release inhibitors and NMDA receptor antagonists or dampening NMDA function have antidepressant effects in animal models of depression [1, 57-62].

Glutamatergic inputs to CA3 originate from three main sources: the DG via mossy fibers, the entorhinal cortex via the perforant path, and bilateral CA3 itself via associational/commissural pathways [63]. It has been reported that the second input from the entorhinal cortex was not observed in the mouse, at least in the C57BL/6J strain of mice [64]. Thus, the extrinsic glutamatergic inputs to CA3 in C57BL/6J mice, the mouse strain used in this study,

originate primarily from granule neurons in DG [28, 65, 66]. Not surprisingly, granule neurons in DG play critical roles in regulating excitability and plasticity of CA3 neurons [67, 68].

The DG is a unique brain structure where most granule neurons (~95%) are generated early during embryonic and postnatal development [69, 70] and a minor population of neurons (~5%) are produced in adulthood (i.e. adult neurogenesis) [71, 72]. Numerous studies on depressive behaviors and antidepressant actions have focused on adult-born neurons in DG. Adult neurogenesis in DG is increased by chronic administration of antidepressant drugs and suppressed by various forms of stress and in animal models of depression [73-76], leading to the hypothesis that DG neurogenesis is involved in both depression and antidepressant treatment. However, current findings in the field implicate that reduced adult neurogenesis is not sufficient to induce depression, and stimulation of neurogenesis is not likely the sole mechanism of treatment efficacy [77]. Given the time course for new neuron maturation and integration, neurogenesis is unlikely to contribute to rapid antidepressant effects. We have previously shown that hippocampal adult-born new neurons mediate the delayed long-lasting behavioral effect of leptin, but is not necessary for the acute effect of leptin in reversing stress-induced behavioral despair [29], suggesting the important role for existing/mature DG granule neurons in mediating the acute actions leptin [22, 29].

Existing/mature granule neurons in DG are heterogeneous in their electrophysiological and functional properties. Different types of stressors seem to selectively activate a portion of DG granule neurons [33-38]. However, the lack of neurochemical markers has limited a full evaluation of stress-responsive or non-responsive DG neurons. One intriguing finding in this study is that LepRb was expressed in a subpopulation of DG granule neurons, and these neurons were devoid of activation of tail suspension stress and forced swim stress. Similar results were also obtained in mice subjected to social defeat (data not shown). These observations led us to hypothesize that there may exist two distinct populations of DG granule neurons; one for encoding stress reactivity and driving excitatory transmission in CA3 and the other for exerting anti-stress/antidepressant activity and dampening excitatory transmission in CA3. Our results suggest that leptin is likely to dampen NMDA-mediated excitatory transmission in CA3. Interestingly, it has been recently reported that ghrelin, a gut hormone, regulates excitatory synaptic transmission in CA1 via another glutamate receptor, the AMPA receptor [78]. Together, these studies support a link between metabolic control and hippocampal neuronal function.

One question arises as to how LepRb neurons in DG regulate stress-evoked glutamate release in CA3? One possibility is that activation of LepRb granule neurons recruit local inhibitory interneurons to suppress stress-activated excitatory granule neurons. Studies have shown that the mossy fiber axons arising from granule neurons give rise to collaterals that heavily innervate GABAergic interneurons and excite these neurons in DG [79, 80]. The widely distributed axonal plexus of interneurons would allow a single GABAergic interneuron to influence a very large number of glutamatergic granule cells [81]. Another possibility is that activation of DG LepRb neurons recruits GABAergic interneurons in CA3, which then inhibit glutamate release from commissual/associational CA3 synapses [63]. It has been shown that the axons of DG granule neurons can synapse with both pyramidal neurons and interneurons in CA3 [82-84]. We propose that LepRb neurons exert their effects on

behavioral despair via inhibiting stress-responsive granule neurons in DG or dampening stress-induced glutamate release/transmission in CA3. This is supported by our finding that inhibition of Akt signaling in DG blocked the antidepressant-like effect of i.p. injection of leptin. However, the possibility of leptin actions on glutamate release in CA3 via LepRb neruons that lie outside the DG cannot be excluded. Future studies will investigate whether LepRb neurons in DG are a common target of anti-stress and antidepressant agents.

Conclusion

Our data suggest that behavioral despair involves glutamate release and NMDA receptor-mediated transmission in CA3. The DG, a structure positioned at the entrance of the hippocampal tri-synaptic circuit, integrates stress and anti-stress signals, exert spatial and temporal modifications to the DG-CA3 excitatory circuitry and thereby control behavioral outputs. Abnormal development and dysfunction of the DG-CA3 pathway and glutamatergic synaptic transmission are thought to contribute to the pathogenesis of depression and other psychiatric disorders. Our findings of leptin modulation of the DG-CA3 glutamatergic pathway suggest novel therapeutic strategies for treatment of psychiatric disorders.

ACKNOWLEDGEMENTS

REFERENCES

1. Skolnick P, Popik P, Trullas R. Glutamate-based antidepressants: 20 years on. Trends Pharmacol Sci. 2009; 30(11):563–569. [PubMed: 19837463]

2. Zarate C Jr. Machado-Vieira R, Henter I, Ibrahim L, Diazgranados N, Salvadore G. Glutamatergic modulators: the future of treating mood disorders? Harv Rev Psychiatry. 2010; 18(5):293–303. [PubMed: 20825266]

3. Krystal JH, Sanacora G, Duman RS. Rapid-acting glutamatergic antidepressants: the path to ketamine and beyond. Biol Psychiatry. 73(12):1133–1141. [PubMed: 23726151]

4. Lowy MT, Gault L, Yamamoto BK. Adrenalectomy attenuates stress-induced elevations in extracellular glutamate concentrations in the hippocampus. J Neurochem. 1993; 61(5):1957–1960. [PubMed: 7901339]

5. Lowy MT, Wittenberg L, Yamamoto BK. Effect of acute stress on hippocampal glutamate levels and spectrin proteolysis in young and aged rats. J Neurochem. 1995; 65(1):268–274. [PubMed: 7790870]

6. Moghaddam B. Stress preferentially increases extraneuronal levels of excitatory amino acids in the prefrontal cortex: comparison to hippocampus and basal ganglia. J Neurochem. 1993; 60(5):1650–1657. [PubMed: 8097232]

7. Bagley J, Moghaddam B. Temporal dynamics of glutamate efflux in the prefrontal cortex and in the hippocampus following repeated stress: effects of pretreatment with saline or diazepam. Neuroscience. 1997; 77(1):65–73. [PubMed: 9044375]

8. Musazzi L, Milanese M, Farisello P, Zappettini S, Tardito D, Barbiero VS, et al. Acute stress increases depolarization-evoked glutamate release in the rat prefrontal/frontal cortex: the dampening action of antidepressants. PLoS One. 2010; 5(1):e8566. [PubMed: 20052403]

9. Satoh E, Shimeki S. Acute restraint stress enhances calcium mobilization and glutamate exocytosis in cerebrocortical synaptosomes from mice. Neurochem Res. 2010; 35(5):693–701. [PubMed: 20069359]

10. Satoh E, Tada Y, Matsuhisa F. Chronic stress enhances calcium mobilization and glutamate exocytosis in cerebrocortical synaptosomes from mice. Neurol Res. 2011; 33(9):899–907. [PubMed: 22080989]

11. de Vasconcellos-Bittencourt AP, Vendite DA, Nassif M, Crema LM, Frozza R, Thomazi AP, et al. Chronic stress and lithium treatments alter hippocampal glutamate uptake and release in the rat and potentiate necrotic cellular death after oxygen and glucose deprivation. Neurochem Res. 2011; 36(5):793–800. [PubMed: 21253855]

12. Reznikov LR, Grillo CA, Piroli GG, Pasumarthi RK, Reagan LP, Fadel J. Acute stress-mediated increases in extracellular glutamate levels in the rat amygdala: differential effects of antidepressant treatment. Eur J Neurosci. 2007; 25(10):3109–3114. [PubMed: 17561824]

13. Macqueen G, Frodl T. The hippocampus in major depression: evidence for the convergence of the bench and bedside in psychiatric research? Mol Psychiatry. 2011; 16(3):252–264. [PubMed: 20661246]

14. Campbell S, Macqueen G. The role of the hippocampus in the pathophysiology of major depression. J Psychiatry Neurosci. 2004; 29(6):417–426. [PubMed: 15644983]

15. Sapolsky RM. Depression, antidepressants, and the shrinking hippocampus. Proc Natl Acad Sci U S A. 2001; 98(22):12320–12322. [PubMed: 11675480]

16. Sheline YI. Hippocampal atrophy in major depression: a result of depression-induced neurotoxicity? Mol Psychiatry. 1996; 1(4):298–299. [PubMed: 9118352]

17. Frodl T, Meisenzahl EM, Zetzsche T, Born C, Groll C, Jager M, et al. Hippocampal changes in patients with a first episode of major depression. Am J Psychiatry. 2002; 159(7):1112–1118. [PubMed: 12091188]

18. Mayberg HS, Brannan SK, Tekell JL, Silva JA, Mahurin RK, McGinnis S, et al. Regional metabolic effects of fluoxetine in major depression: serial changes and relationship to clinical response. Biol Psychiatry. 2000; 48(8):830–843. [PubMed: 11063978]

19. McEwen BS. Stress and hippocampal plasticity. Annu Rev Neurosci. 1999; 22:105–122. [PubMed: 10202533]

20. Adachi M, Barrot M, Autry AE, Theobald D, Monteggia LM. Selective loss of brain-derived neurotrophic factor in the dentate gyrus attenuates antidepressant efficacy. Biol Psychiatry. 2008; 63(7):642–649. [PubMed: 17981266]

21. Guo M, Lu Y, Garza JC, Li Y, Chua SC, Zhang W, et al. Forebrain glutamatergic neurons mediate leptin action on depression-like behaviors and synaptic depression. Transl Psychiatry. 2012; 2:e83. [PubMed: 22408745]

22. Lu XY, Kim CS, Frazer A, Zhang W. Leptin: a potential novel antidepressant. Proc Natl Acad Sci U S A. 2006; 103(5):1593–1598. [PubMed: 16423896]

23. Omata N, Chiu CT, Moya PR, Leng Y, Wang Z, Hunsberger JG, et al. Lentivirally mediated GSK-3beta silencing in the hippocampal dentate gyrus induces antidepressant-like effects in stressed mice. Int J Neuropsychopharmacol. 2010:1–7.

24. Shirayama Y, Chen AC, Nakagawa S, Russell DS, Duman RS. Brain-derived neurotrophic factor produces antidepressant effects in behavioral models of depression. J Neurosci. 2002; 22(8):3251–3261. [PubMed: 11943826]

25. McKittrick CR, Magarinos AM, Blanchard DC, Blanchard RJ, McEwen BS, Sakai RR. Chronic social stress reduces dendritic arbors in CA3 of hippocampus and decreases binding to serotonin transporter sites. Synapse. 2000; 36(2):85–94. [PubMed: 10767055]

26. Watanabe Y, Gould E, McEwen BS. Stress induces atrophy of apical dendrites of hippocampal CA3 pyramidal neurons. Brain Res. 1992; 588(2):341–345. [PubMed: 1393587]

27. Christian, Kimberly M.; Miracle, Angela D.; Wellman, Cara L.; Nakazawa, K. Chronic stress-induced hippocampal dendritic retraction requires CA3 NMDA receptors. Neuroscience. 2011; (174):26–36. [PubMed: 21108993]

28. Claiborne BJ AD, Cowan WM. A light and electron microscopic analysis of the mossy fibers of the rat dentate gyrus. J Comp Neurol. 1986; 246(4):435–458. [PubMed: 3700723]

29. Garza JC, Guo M, Zhang W, Lu XY. Leptin restores adult hippocampal neurogenesis in a chronic unpredictable stress model of depression and reverses glucocorticoid-induced inhibition of GSK-3beta/beta-catenin signaling. Mol Psychiatry. 2012; 17(8):790–808. [PubMed: 22182938]

30. Lu XY. The leptin hypothesis of depression: a potential link between mood disorders and obesity? Curr Opin Pharmacol. 2007; 7(6):648–652. [PubMed: 18032111]

31. Yamada N, Katsuura G, Ochi Y, Ebihara K, Kusakabe T, Hosoda K, et al. Impaired CNS leptin action is implicated in depression associated with obesity. Endocrinology. 2011; 152(7):2634–2643. [PubMed: 21521746]

32. Guo M, Huang TY, Garza JC, Chua SC, Lu XY. Selective deletion of leptin receptors in adult hippocampus induces depression-related behaviours. Int J Neuropsychopharmacol. 2013; 16(4):857–867. [PubMed: 22932068]

33. Sharp FR, Sagar SM, Hicks K, Lowenstein D, Hisanaga K. c-fos mRNA, Fos, and Fos-related antigen induction by hypertonic saline and stress. J Neurosci. 1991; 11(8):2321–2331. [PubMed: 1908006]

34. Katano H, Masago A, Yamada K. Marked alteration of c-fos and c-jun but not hsp70 messenger RNA expression in rat brain after cold-induced trauma: An in situ hybridization study. Restor Neurol Neurosci. 1997; 11(3):153–160. [PubMed: 21551539]

35. Chandramohan Y, Droste SK, Reul JM. Novelty stress induces phospho-acetylation of histone H3 in rat dentate gyrus granule neurons through coincident signalling via the N-methyl-D-aspartate receptor and the glucocorticoid receptor: relevance for c-fos induction. J Neurochem. 2007; 101(3):815–828. [PubMed: 17250652]

36. Chandramohan Y, Droste SK, Arthur JS, Reul JM. The forced swimming-induced behavioural immobility response involves histone H3 phospho-acetylation and c-Fos induction in dentate gyrus granule neurons via activation of the N-methyl-D-aspartate/extracellular signal-regulated kinase/mitogen- and stress-activated kinase signalling pathway. Eur J Neurosci. 2008; 27(10):2701–2713. [PubMed: 18513320]

37. Fevurly RD, Spencer RL. Fos expression is selectively and differentially regulated by endogenous glucocorticoids in the paraventricular nucleus of the hypothalamus and the dentate gyrus. J Neuroendocrinol. 2004; 16(12):970–979. [PubMed: 15667452]

38. Schoenfeld TJ, Rada P, Pieruzzini PR, Hsueh B, Gould E. Physical exercise prevents stress-induced activation of granule neurons and enhances local inhibitory mechanisms in the dentate gyrus. J Neurosci. 33(18):7770–7777.

39. Porsolt RD, Le Pichon M, Jalfre M. Depression: a new animal model sensitive to antidepressant treatments. Nature. 1977; 266(5604):730–732. [PubMed: 559941]

40. Steru L, Chermat R, Thierry B, Simon P. The tail suspension test: a new method for screening antidepressants in mice. Psychopharmacology (Berl). 1985; 85(3):367–370. [PubMed: 3923523]

41. DeFalco J, Tomishima M, Liu H, Zhao C, Cai X, Marth JD, et al. Virus-assisted mapping of neural inputs to a feeding center in the hypothalamus. Science. 2912001:2608–2613.

42. Liu J, Perez SM, Zhang W, Lodge DJ, Lu XY. Selective deletion of the leptin receptor in dopamine neurons produces anxiogenic-like behavior and increases dopaminergic activity in amygdala. Mol Psychiatry. 2011; 16(10):1024–1038. [PubMed: 21483433]

43. Liu J, Guo M, Zhang D, Cheng SY, Liu M, Ding J, et al. Adiponectin is critical in determining susceptibility to depressive behaviors and has antidepressant-like activity. Proc Natl Acad Sci U S A. 2012; 109(30):12248–12253. [PubMed: 22778410]

44. George Paxinos, KBJF. The Mouse Brain in Stereotaxic Coordinates. 3th edn.. Elsevier; 2008. p. 242

45. Hardingham GE, Fukunaga Y, Bading H. Extrasynaptic NMDARs oppose synaptic NMDARs by triggering CREB shut-off and cell death pathways. Nat Neurosci. 2002; 5(5):405–414. [PubMed: 11953750]

46. Marsden WN. Stressor-induced NMDAR dysfunction as a unifying hypothesis for the aetiology, pathogenesis and comorbidity of clinical depression. Med Hypotheses. 2011; 77(4):508–528. [PubMed: 21741771]

47. Shaner NC, Patterson GH, Davidson MW. Advances in fluorescent protein technology. J Cell Sci. 2007; 120(Pt 24):4247–4260. [PubMed: 18057027]

48. Madisen L, Zwingman TA, Sunkin SM, Oh SW, Zariwala HA, Gu H, et al. A robust and high-throughput Cre reporting and characterization system for the whole mouse brain. Nat Neurosci. 2010; 13(1):133–140. [PubMed: 20023653]

49. Duman RS, Li N, Liu RJ, Duric V, Aghajanian G. Signaling pathways underlying the rapid antidepressant actions of ketamine. Neuropharmacology. 2012; 62(1):35–41. [PubMed: 21907221]

50. Niswender KD, Morton GJ, Stearns WH, Rhodes CJ, Myers MG Jr. Schwartz MW. Intracellular signalling. Key enzyme in leptin-induced anorexia. Nature. 2001; 413(6858):794–795. [PubMed: 11677594]

51. Yamamoto B, Reagan LP. The glutamatergic system in neuronal plasticity and vulnerability in mood disorders. Neuropsych Dis Treat. 2006; 2(Suppl. 2):7–14.

52. Bonanno G, Giambelli R, Raiteri L, Tiraboschi E, Zappettini S, Musazzi L, et al. Chronic antidepressants reduce depolarization-evoked glutamate release and protein interactions favoring formation of SNARE complex in hippocampus. J Neurosci. 2005; 25(13):3270–3279. [PubMed: 15800181]

53. Milanese M, Tardito D, Musazzi L, Treccani G, Mallei A, Bonifacino T, et al. Chronic treatment with agomelatine or venlafaxine reduces depolarization-evoked glutamate release from hippocampal synaptosomes. BMC Neurosci. 2013; 14(75)

54. Barks JD, Silverstein FS, Sims K, Greenamyre JT, MV. J. Glutamate recognition sites in human fetal brain. Neurosci Lett. 1988; 84(2):131–136. [PubMed: 2893319]

55. Vizi ES, Fekete A, Karoly R, A. M. Non-synaptic receptors and transporters involved in brain functions and targets of drug treatment. Br J Pharmacol. 2010; 160(4):785–809. [PubMed: 20136842]

56. Hardingham GE, Bading H. Synaptic versus extrasynaptic NMDA receptor signalling: implications for neurodegenerative disorders. Nat Rev Neurosci. 2010; 11(10):682–696. [PubMed: 20842175]

57. Berman RM, Cappiello A, Anand A, Oren DA, Heninger GR, Charney DS, et al. Antidepressant effects of ketamine in depressed patients. Biol Psychiatry. 2000; 47(4):351–354. [PubMed: 10686270]

58. Diazgranados N, Ibrahim L, Brutsche NE, Newberg A, Kronstein P, Khalife S, et al. A randomized add-on trial of an N-methyl-D-aspartate antagonist in treatment-resistant bipolar depression. Arch Gen Psychiatry. 2010; 67(8):793–802. [PubMed: 20679587]

59. Preskorn SH, Baker B, Kolluri S, Menniti FS, Krams M, Landen JW. An innovative design to establish proof of concept of the antidepressant effects of the NR2B subunit selective N-methyl-D-aspartate antagonist, CP-101,606, in patients with treatment-refractory major depressive disorder. J Clin Psychopharmacol. 2008; 28(6):631–637. [PubMed: 19011431]

60. Zarate CA Jr. Singh JB, Carlson PJ, Brutsche NE, Ameli R, Luckenbaugh DA, et al. A randomized trial of an N-methyl-D-aspartate antagonist in treatment-resistant major depression. Arch Gen Psychiatry. 2006; 63(8):856–864. [PubMed: 16894061]

61. Skolnick P, Layer RT, Popik P, Nowak G, Paul IA, Trullas R. Adaptation of N-methyl-D-aspartate (NMDA) receptors following antidepressant treatment: implications for the pharmacotherapy of depression. Pharmacopsychiatry. 1996; 29(1):23–26. [PubMed: 8852530]

62. Popoli M, Yan Z, McEwen BS, Sanacora G. The stressed synapse: the impact of stress and glucocorticoids on glutamate transmission. Nat Rev Neurosci. 2011; 13(1):22–37. [PubMed: 22127301]

63. Witter. M. Intrinsic and extrinsic wiring of CA3: indications for connectional heterogeneity. Learn Mem. 2007; 14(11):705–713. [PubMed: 18007015]

64. van Groen T, Miettinen P, I. K. The entorhinal cortex of the mouse: organization of the projection to the hippocampal formation. Hippocampus. 2003; 13(1):133–149. [PubMed: 12625464]

65. Blackstad TW BK, Hem J, Jeune B. Distribution of hippocampal mossy fibers in the rat. An experimental study with silver impregnation methods. J Comp Neurol. 1970; 138(4):433–449. [PubMed: 4907846]

66. Swanson LW WJ, Cowan WM. An autoradiographic study of the organization of intrahippocampal association pathways in the rat. J Comp Neurol. 1978; 181(4):681–715. [PubMed: 690280]

67. Kobayashi K, Poo MM. Spike train timing-dependent associative modification of hippocampal CA3 recurrent synapses by mossy fibers. Neuron. 2004; 41(3):445–454. [PubMed: 14766182]

68. Henze DA, Wittner L, Buzsaki G. Single granule cells reliably discharge targets in the hippocampal CA3 network in vivo. Nat Neurosci. 2002; 5(8):790–795. [PubMed: 12118256]

69. Schlessinger AR, Cowan WM, Gottlieb DI. An autoradiographic study of the time of origin and the pattern of granule cell migration in the dentate gyrus of the rat. J Comp Neurol. 1975; 159(2):149–175. [PubMed: 1112911]

70. Altman J, Bayer SA. Migration and distribution of two populations of hippocampal granule cell precursors during the perinatal and postnatal periods. J Comp Neurol. 1990; 301(3):365–381. [PubMed: 2262596]

71. Eriksson PS, Perfilieva E, Bjork-Eriksson T, Alborn AM, Nordborg C, Peterson DA, et al. Neurogenesis in the adult human hippocampus. Nat Med. 1998; 4(11):1313–1317. [PubMed: 9809557]

72. Gould E, Tanapat P. Stress and hippocampal neurogenesis. Biol Psychiatry. 1999; 46(11):1472–1479. [PubMed: 10599477]

73. Kempermann G, Kronenberg G. Depressed new neurons--adult hippocampal neurogenesis and a cellular plasticity hypothesis of major depression. Biol Psychiatry. 2003; 54(5):499–503. [PubMed: 12946878]

74. Warner-Schmidt JL, Duman RS. Hippocampal neurogenesis: opposing effects of stress and antidepressant treatment. Hippocampus. 2006; 16(3):239–249. [PubMed: 16425236]

75. Malberg JE, Eisch AJ, Nestler EJ, Duman RS. Chronic antidepressant treatment increases neurogenesis in adult rat hippocampus. J Neurosci. 2000; 20(24):9104–9110. [PubMed: 11124987]

76. Sahay A, Drew MR, Hen R. Dentate gyrus neurogenesis and depression. Prog Brain Res. 2007; 163:697–722. [PubMed: 17765746]

77. David DJ, Samuels BA, Rainer Q, Wang JW, Marsteller D, Mendez I, et al. Neurogenesis-dependent and -independent effects of fluoxetine in an animal model of anxiety/depression. Neuron. 2009; 62(4):479–493. [PubMed: 19477151]

78. Ribeiro LF, Catarino T, Santos SD, Benoist M, van Leeuwen JF, Esteban JA, et al. Ghrelin triggers the synaptic incorporation of AMPA receptors in the hippocampus. Proc Natl Acad Sci U S A. 111(1):E149–158. [PubMed: 24367106]

79. Ribak CE. Axon terminals of GABAergic chandelier cells are lost at epileptic foci. Brain Res. 1985; 326(2):251–260. [PubMed: 2982461]

80. Acsady L, Kamondi A, Sik A, Freund T, Buzsaki G. GABAergic cells are the major postsynaptic targets of mossy fibers in the rat hippocampus. J Neurosci. 1998; 18(9):3386–3403. [PubMed: 9547246]

81. Scharfman, H., editor. The Dentate Gyrus: A Comprehensive Guide to Structure, Function, and Clinical Implications. Elsevier Science; 2007.

82. Lawrence JJ, McBain CJ. Interneuron diversity series: containing the detonation--feedforward inhibition in the CA3 hippocampus. Trends Neurosci. 2003; 26(11):631–640. [PubMed: 14585604]

83. Pelkey KA, McBain CJ. Target-cell-dependent plasticity within the mossy fibre-CA3 circuit reveals compartmentalized regulation of presynaptic function at divergent release sites. J Physiol. 2008; 586(6):1495–1502. [PubMed: 18079156]

84. Toth K, Suares G, Lawrence JJ, Philips-Tansey E, McBain CJ. Differential mechanisms of transmission at three types of mossy fiber synapse. J Neurosci. 2000; 20(22):8279–8289. [PubMed: 11069934]
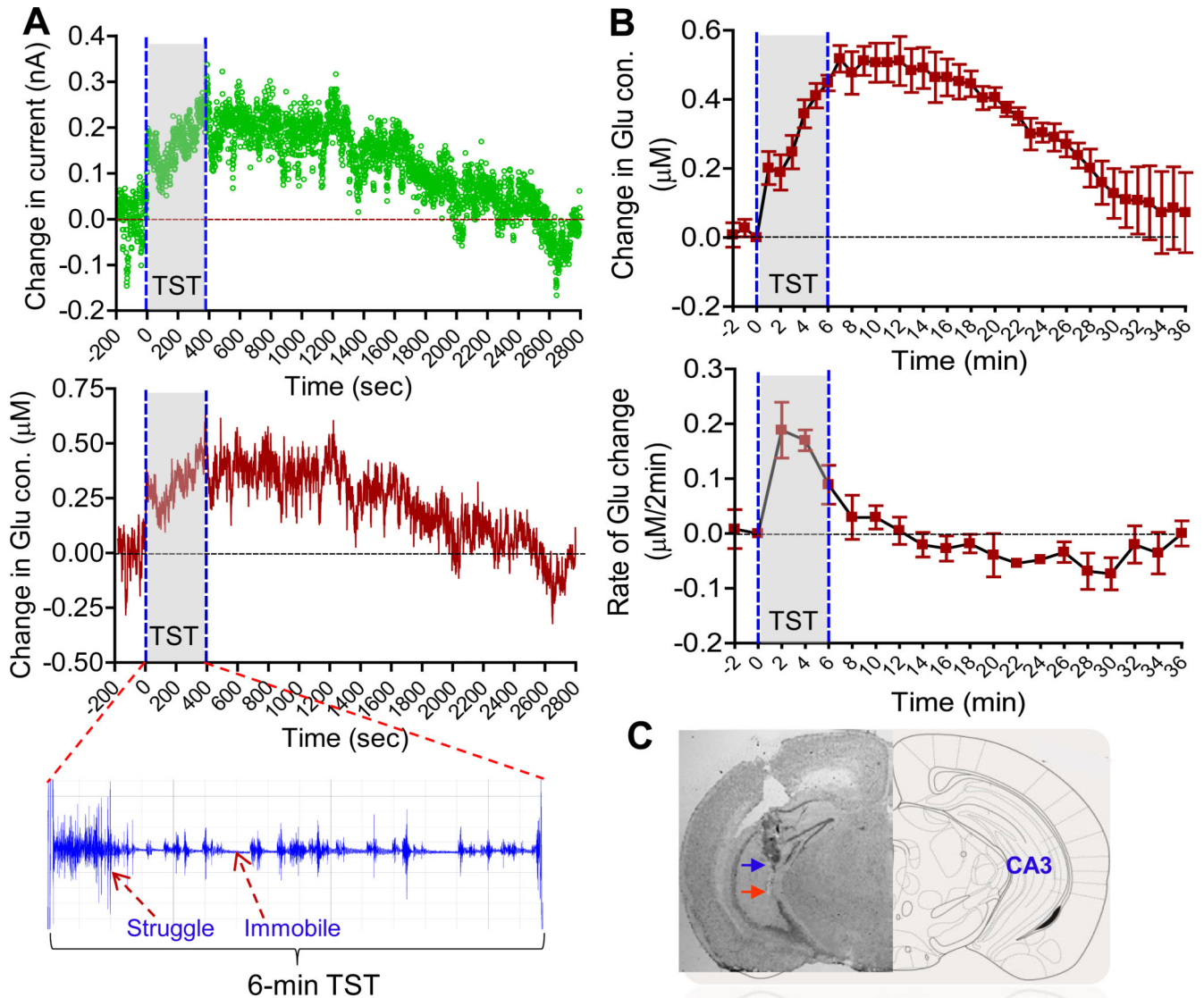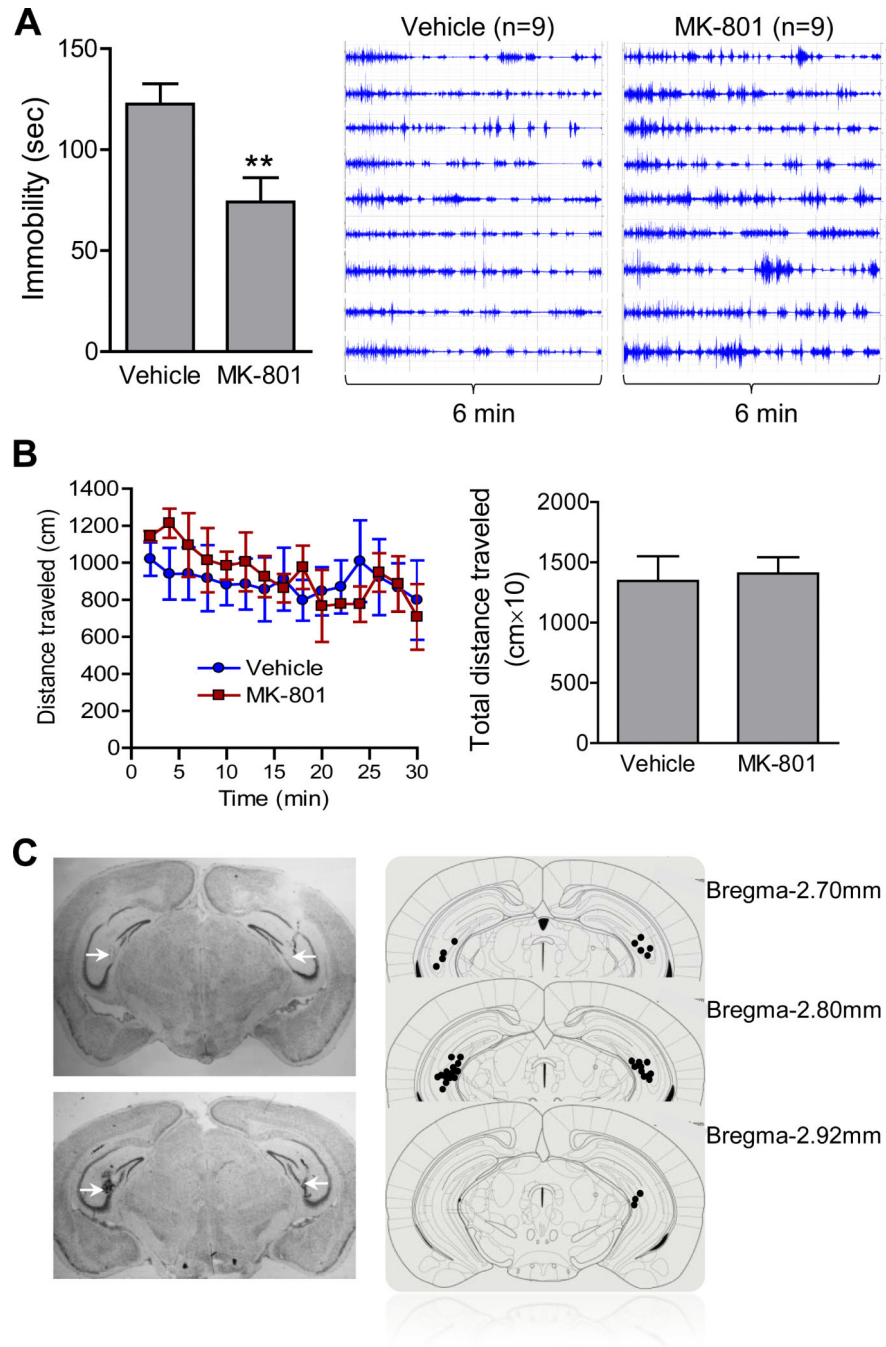
Figure 1.
Real-time changes in extracellular glutamate concentrations in CA3 induced by tail suspension. Extracellular electrical currents were recorded by glutamate-sensitive micro-biosensors implanted in the CA3 and converted to glutamate concentrations. **A**. Top, a representative electrical current trace recorded at 1Hz by a biosensor after tail suspension (grey area); middle, changes in extracellular glutamate (Glu) concentrations (1-min bin); bottom, histogram of behavioral responses, 'struggle' and 'immobile' episodes, during 6-min tail suspension. **B**. Top, extracellular glutamate concentrations (1-min bin) in the CA3 in response to tail suspension. Bottom, rate of change in extracellular glutamate concentrations (2-min bin). n = 4. **C**. Histological verification of biosensor placement. Black arrow indicating the end of the guide cannula; red arrow indicating the tip of the biosensor with an active length of 1 mm. TST, tail suspension test.

Figure 2.
Effects of intra-CA3 injection of the NMDA receptor antagonist MK-801 on behavioral despair in the tail suspension test. MK-801 (1.0 μg) or vehicle was infused bilaterally into the CA3 30 min prior to the tail suspension test or the locomotion test. **A**. Left, immobility time during the tail suspension test scored by video analysis; right, individual histograms showing temporal courses of 'struggle' and 'immobile' episodes during the test following intra-CA3 injection of vehicle or MK-801. n = 9/group. ***P* < 0.01. **B**. Locomotor activity.

Left, distance travelled in 2-min bin; right, total distance traveled within 30 min. n = 4/ group. **C**. Histological verification of injection sites in the CA3.
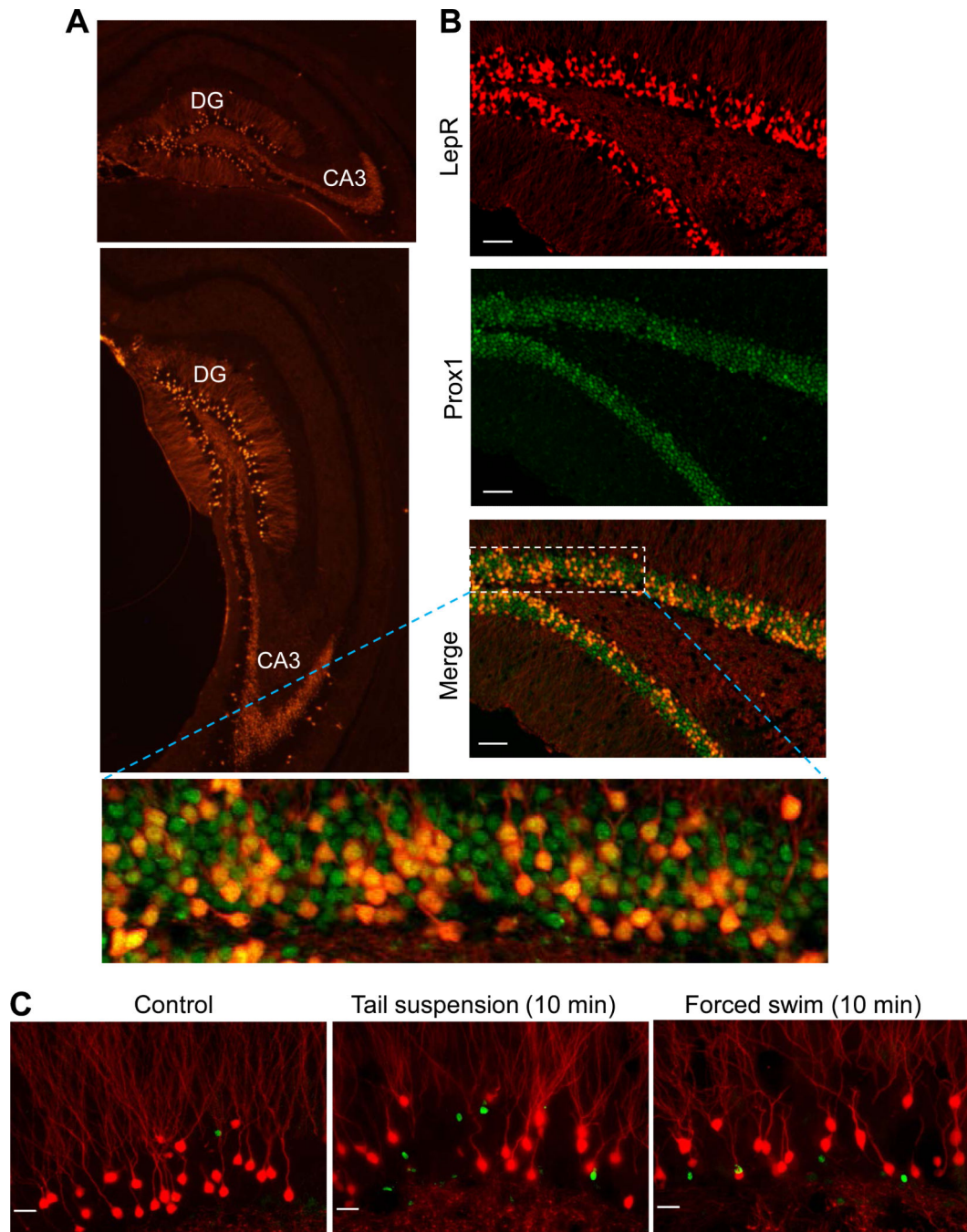
Figure 3.
Distribution of LepRb cells in the hippocampus and effect of leptin on glutamate release in
CA3. **A**. LepRb-tdTomato cells are largely restricted to the granule cell layer of the dentate
gyrus (DG) and extend axonal projections to the CA3 region. **B**. Fluorescent
immunohistochemistry showing the exclusive colocalization of LepRb-tdTomato with
Prox1, a marker of granule neurons, in DG. **C.** c-Fos expression (green) in LepRb-tdTomato
granule cells (red) following 10-min tail suspension or forced swim. Sale bars = 50 μm in B
and 20 μm in C.
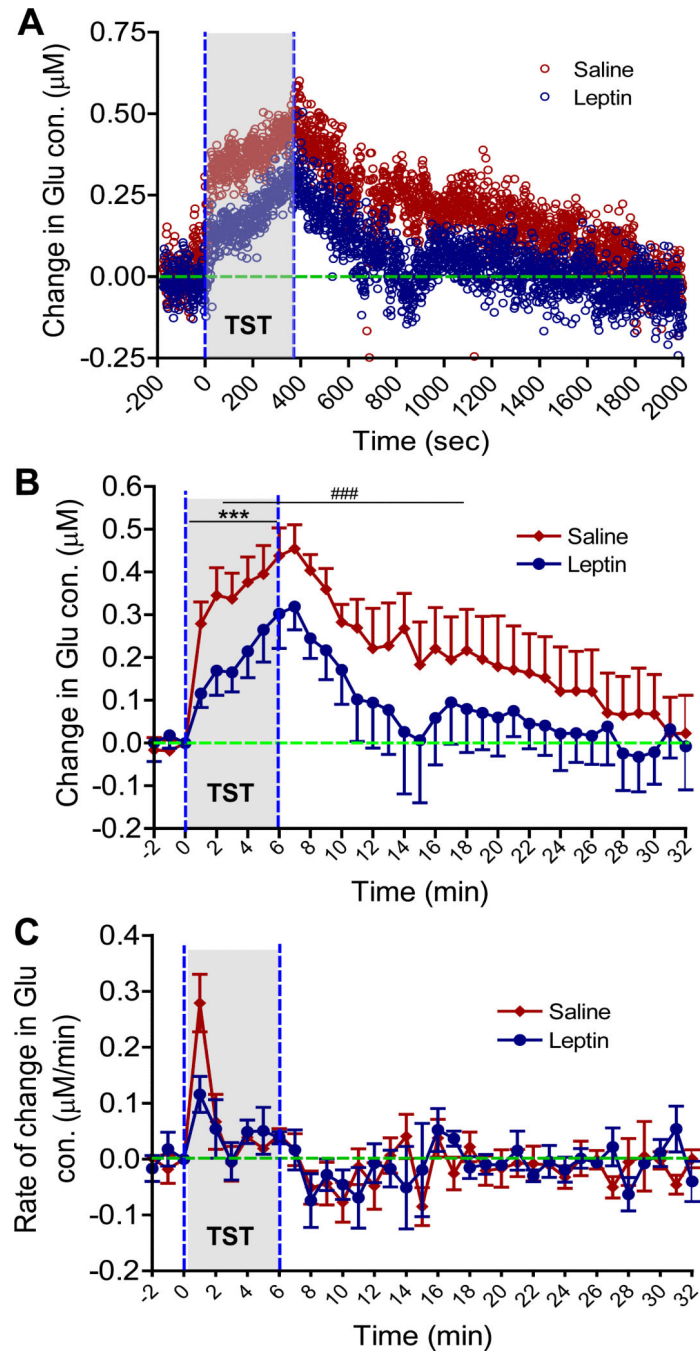
Figure 4.
Effect of leptin on tail suspension-evoked glutamate release in CA3. Leptin (1.0 mg/kg) or saline was injected intraperitoneally into the mice 30 min before tail suspension. **A.** Compositing changes in extracellular glutamate concentrations (μM) converted from current recording at a 1 Hz sampling frequency from 5 saline-treated mice (red open circle) and 4 leptin-treated mice (blue open circle). **B.** Temporal changes in glutamate concentrations in 1-min bin. **C.** Rate of change in glutamate concentrations (μM/min). n = 4-5/group. ***$P <$

0.001 compared to saline-treated controls during 6-min tail suspension. $^{###}P < 0.001$ indicating significant overall difference between two treatment groups.
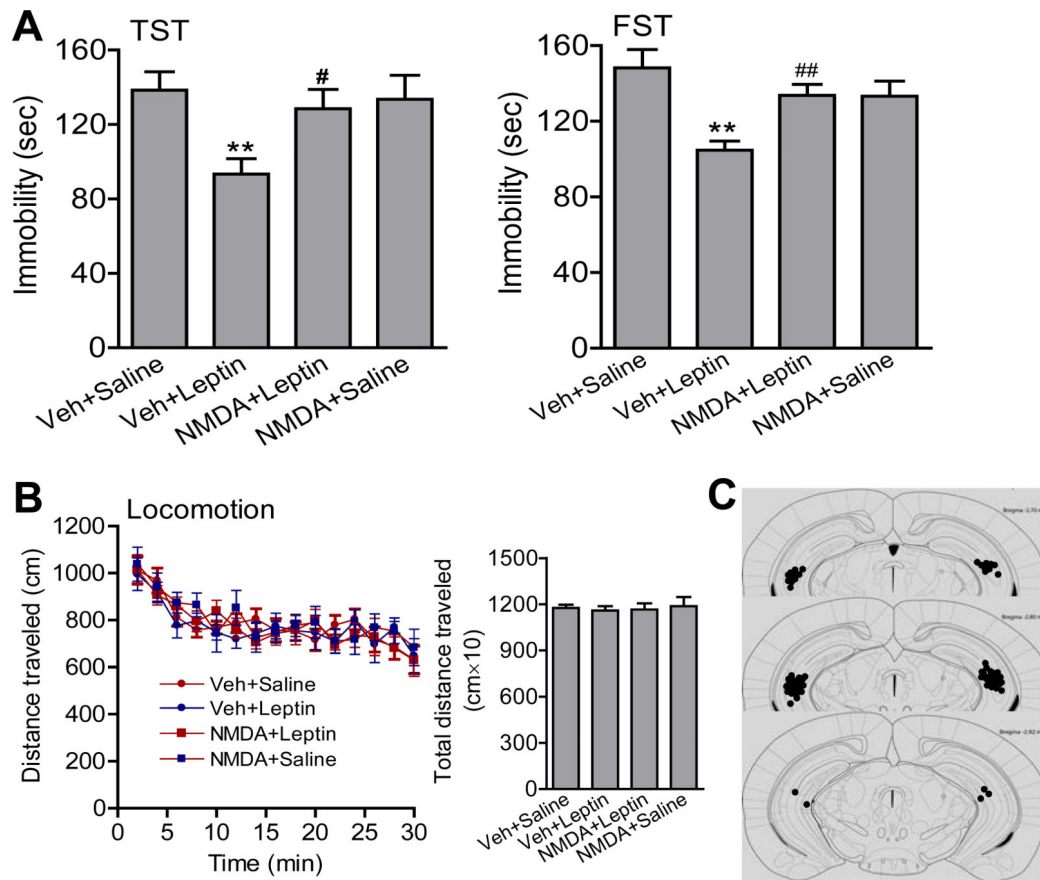
Figure 5.
Intra-CA3 microinjection of NMDA blocks leptin-induced 'anti-despair' effect. Mice received intra-CA3 injection of vehicle or 0.1 nmol NMDA 30 min prior to leptin (1.0 mg/kg, i.p.) or saline injection. The tail suspension test and forced swim test were performed 30 min after leptin injection. **A**. Left panel, tail suspension test (TST); right panel, forced swim test (FST). **B**. Locomotor activity. Left panel, distance traveled in 2-min bins for 30 min; right panel, total distance traveled in 30 min. **C**. Histology of injection sites. **$P < 0.01$ compared with veh-saline group; #$P < 0.05$, ##$P < 0.01$ compared with veh-leptin group.
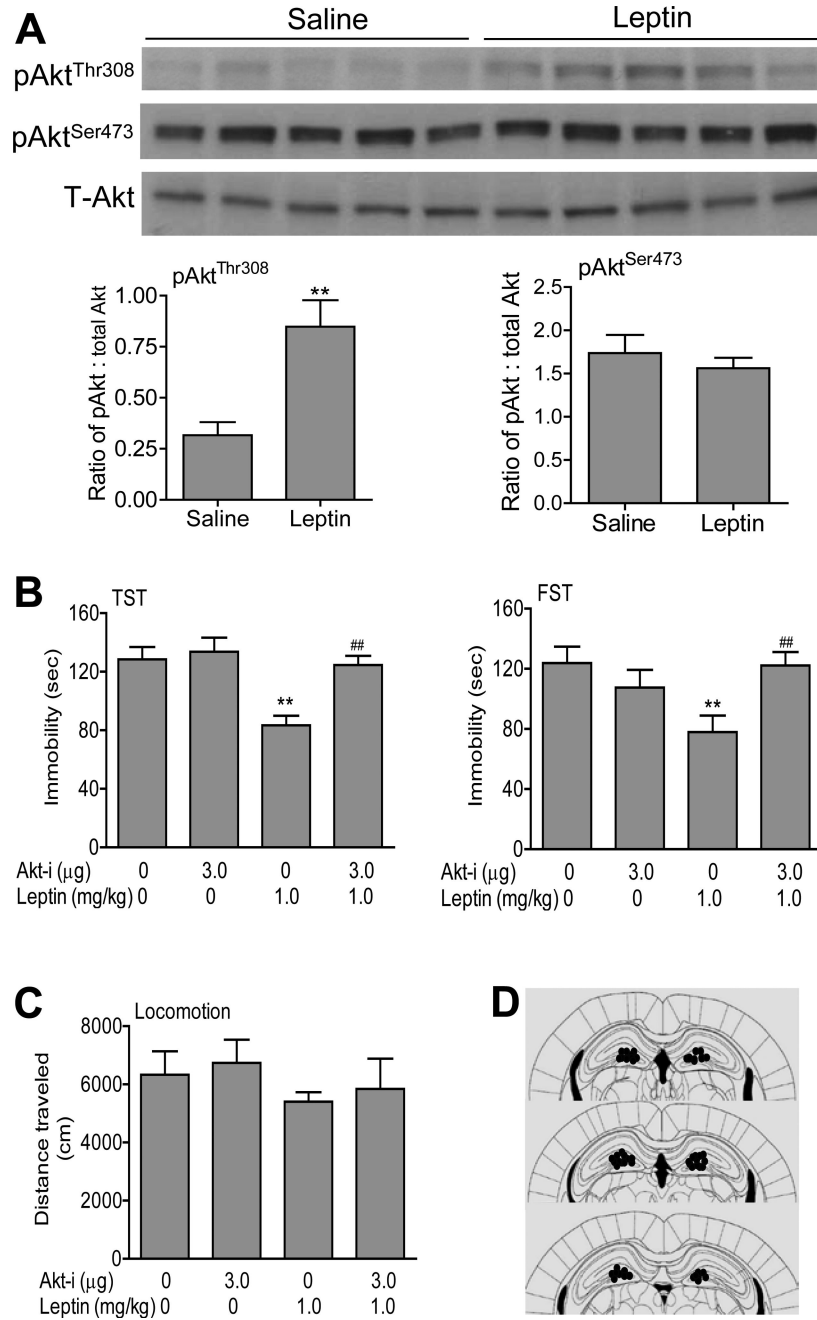
Figure 6.
Akt signaling in the dentate gyrus mediates the effect of leptin on behavioral despair. A. Western blot showing phosphorylated Akt^{Thr308} and Akt^{Ser473} as well as total Akt. Leptin (1.0 mg/kg, i.p.) or saline was given to the mice 30 min before the hippocampi were dissected for immunoblotting. n = 5/group, **$P < 0.01$ compared with saline-treated controls. **B**. Intra-DG infusion of Akt inhibitor VIII (Akt-i) blocks leptin-induced 'anti-despair' effect. Akt inhibitor VIII was infused into the dentate gyrus 30 min prior to leptin treatment (1.0 mg/kg, i.p.). Left panel, tail suspension test (TST); right panel, forced swim

test (FST). **$P < 0.01$ compared with the veh-saline group; [##]$P < 0.01$ compared with veh-leptin group. **C**. Locomotor activity. **D**. Histology of injection sites.